

# Isotope shifts of $6s5d\ ^3D$ -states in neutral barium

U. Dammalapati<sup>a</sup>, S. De, K. Jungmann, and L. Willmann

Kernfysisch Versneller Instituut, University of Groningen, Zernikelaan 25, 9747 AA Groningen, The Netherlands

May 30, 2018

**Abstract.** Laser spectroscopy of the low lying  $^1P$  and  $^3D$  states in atomic barium has been performed. This work contributes substantially to the development of an effective laser cooling and trapping for heavy alkaline earth elements and aims in particular for a better understanding of the atomic wave function of these systems. Isotope shifts and hyperfine structures are ideal probes for the wave functions at the position of the nucleus. This is essential input for a theoretical evaluation of the sensitivity to fundamental symmetry breaking properties like permanent electric dipole moments. We report the first isotope shift measurements of the  $^3D_{1,2}-^1P_1$  transitions. A deviation of the King plot from its expected behavior has been observed. Further we have optically resolved the hyperfine structure of the  $^3D_{1,2}$  states.

**PACS.** 4 2.62.Fi, 39.30.+w, 32.80.Pj

## 1 Introduction

Recently heavy alkaline earth atoms have attracted attention due to high enhancement factors for possible permanent electric dipole moment (edm's), both of electrons and nuclei in several isotopes which have nuclear spin. Of particular interest are radium (Ra) isotopes which exhibit the largest known enhancement factors for an electron edm and for nucleon edm in nuclei. These arise from close lying states of opposite parity [1,2] in the atomic shell ( $^3P$  and  $^3D$ ) or in the nucleus where they are associated with octopole deformations in some nuclei near the region of the valley of stability [3,4]. In order to conduct such research a good understanding of the atomic structure, i.e. wave functions, transition probabilities, lifetimes, and hyperfine structure splitting, is needed. At this time atomic structure calculations with independent numerical approaches are underway [5].

Sensitive experiments with rare or radioactive isotopes such as Ra require samples of laser cooled and trapped atoms. Experiments are prepared at Argonne National Laboratory, IL, USA [6] and at the TRI $\mu$ P facility at the Kernfysisch Versneller Instituut, The Netherlands [7,8]. The development of an effective method for laser cooling and trapping is indispensable. Elaborate laser cooling schemes need to be explored. They involve several lasers at the same time. Barium (Ba), a chemical homologue to Ra, has a similar level structure and is well suited for the development of the technical method due to the copious availability of a large number of stable isotopes.

In atomic Ba, the  $6s^2\ ^1S_0 - 6s6p\ ^1P_1$  transition (Fig. 1) is the strongest transition. It is the only option for laser cooling and trapping in the ground state. The upper state

branches into the  $6s5d\ ^1D_2$ ,  $^3D_2$  and  $^3D_1$  states. This transition has been exploited in the past successfully to determine nuclear magnetic moments and isotope shifts [9]. The level scheme of Ba (Fig. 1) is characterized by low lying  $^1D$  and  $^3D$ -states. This causes a rather large decay of the  $^1P_1$  state into all of these states and puts a strong constraint on the optical cooling cycles. The known transition probabilities (Tab. 1) yields a branching ratio of 1:330(30) for Ba. This value is 1:350(50) for Ra. In contrast, the branching is 1:40000 for the next lighter alkaline earth element strontium, and therefore allows for laser cooling and trapping with a single laser frequency [10].

The similarity in the atomic structure of Ba and Ra allows to work with Ba to establish the experimental techniques and the theoretical framework relevant for searches of edm's in Ra. This paper focusses on the transitions leading to losses from the  $^1S_0-^1P_1$  cooling cycle by branching to metastable D-states. We optically resolved the hyperfine structure of the  $^3D$ -states and measured several isotope shifts. In particular the isotope shifts reveal important correlation effects of the electrons, which are relevant for evaluating enhancement factors for edm's. The developed techniques will allow to perform such measurements with the much less abundant Ra isotopes.

## 2 Experimental approach

An effusive Ba atomic beam is produced from Ba metal at about 800 K in a resistively heated oven. The abundances of naturally occurring Ba isotopes are  $^{138}\text{Ba}$  (71.7%),  $^{137}\text{Ba}$  (11.3%),  $^{136}\text{Ba}$  (7.8%),  $^{135}\text{Ba}$  (6.6%),  $^{134}\text{Ba}$  (2.4%),  $^{132}\text{Ba}$  (0.1%) and  $^{130}\text{Ba}$  (0.1%). The ground state nuclear spin of the even isotopes is zero and for the odd isotopes it is  $3/2\ \hbar$ .

<sup>a</sup> Present address: University of Strathclyde, Glasgow, UK

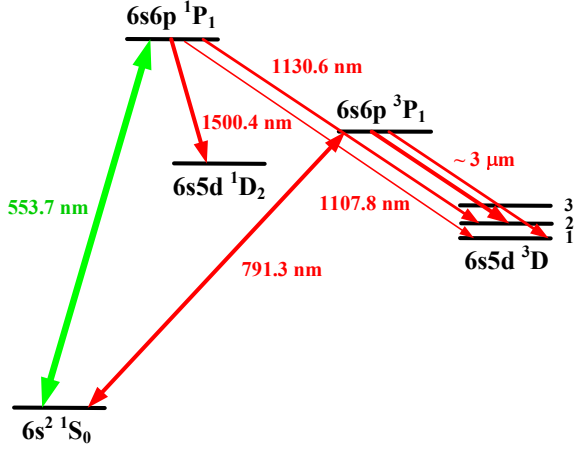


**Fig. 1.** Level diagram of the Ba atom. The wavelengths for the transitions used in laser spectroscopy of the metastable D-states are given.

Upper Level (i)	Lower Level (k)	Label	$\lambda$ [nm]	$A_{ik}$ [ $10^8 \text{ s}^{-1}$ ]
$^1P_1$	$^1S_0$	$\lambda_1$	553.7	$1.19(1)^a$
	$^1D_2$	$\lambda_{ir1}$	1500.4	$0.0025(2)^a$
	$^3D_2$	$\lambda_{ir2}$	1130.6	$0.0011(2)^a$
	$^3D_1$	$\lambda_{ir3}$	1107.8	$0.000031(5)^a$
$^3P_1$	$^1S_0$	$\lambda_2$	791.3	$0.0030(3)$
	$^3D_2$		2923.0	$0.0032(3)^b$
	$^3D_1$		2775.7	$0.0012(1)^b$

**Table 1.** The energy levels, vacuum wavelengths  $\lambda$  and transition rates of the Ba atom relevant for the experiments. Experimental transition rates  $A_{ik}$  are taken from: ‘a’ [11, 12], ‘b’ [13].

State	$^1P_1$	$^1D_2$	$^3D_2$	$^3P_1$
$\tau$	8.2(2)ns[14]	0.25s[15]	60s[15]	1345(14)ns[16]

**Table 2.** Lifetimes of the  $^1P_1$ ,  $^1D_2$ ,  $^3D_2$  and  $^3P_1$  states. The reference [14, 16] quote experimental values and [15] quote calculated values.

The experimental apparatus (Fig. 2) is designed to fulfill two requirements: First, the production of an atomic beam of metastable D-state atoms by optical pumping. Second, infrared laser spectroscopy of the metastable states. The setup provides two separate interaction zones of the atomic beam with laser beams. We observe the transitions originating from the metastable D-states by fluorescence at the wavelength  $\lambda_1$ . In this paper we focus on the  $^3D$  states.

## 2.1 Isotope selective metastable production

Metastable atoms in the D-states are produced by optical pumping with a laser beam orthogonal to the atomic velocity direction. Isotope selective production can be accomplished either by driving the  $6s^2 \ ^1S_0 - 6s6p \ ^1P_1$  transition at wavelength  $\lambda_1 = 553.7 \text{ nm}$  followed by spontaneous

Isotope pair	Isotope shift [MHz] at $\lambda_1$	Isotope shift [MHz] at $\lambda_2$
138-137	-215.15(16)	-183.4(1.0)
138-136	-128.02(39)	-109.2(1.0)
138-135	-259.29(17)	-219.9(1.0)
138-134	-143.0(5)	-122.3(2.5)

**Table 3.** Isotope shifts of the transitions at wavelength  $\lambda_1$  [9] and  $\lambda_2$  [17] in Ba.

decay or by the  $6s^2 \ ^1S_0 - 6s6p \ ^3P_1$  intercombination line at wavelength  $\lambda_2 = 791.3 \text{ nm}$ . The latter possibility allows to populate the  $^3D$ -states exclusively. The isotope shifts (Tab. 3) of these transitions permit isotope selective optical pumping into the metastable state. We use the second option because of the large branching of the  $^3P_1$  state to the  $^3D$ -states (Tab. 1). In addition, the narrow linewidth of the intercombination line at wavelength  $\lambda_2$  allows for a superior isotope selection. Among other transitions, the  $^3D_2 - ^1P_1$  transition at wavelength  $\lambda_{ir2} = 1130.6 \text{ nm}$  and the  $^3D_1 - ^1P_1$  transition at wavelength  $\lambda_{ir3} = 1107.8 \text{ nm}$  have been observed in fluorescence in Fourier transform spectroscopy using a hollow-cathode discharge lamp [11, 12].

We use two home built grating stabilized diode lasers at wavelength  $\lambda_2$ . The Hitachi 7851G laser diodes deliver 15mW each. One reference laser is stabilized against the ‘a1’ line of the P(52)(0-15) transition in molecular iodine  $^{127}\text{I}_2$  by frequency modulation saturated absorption spectroscopy (Fig.4). The second diode laser is frequency offset locked to the iodine stabilized laser. The offset frequency is measured by a beat note on a fast photodiode. The beat frequency for the different isotopes ranges from -3 GHz to 2 GHz because of the large hyperfine structure of the odd isotopes. The light of this second laser frequency shifted by double passing it through an 200 MHz acousto optical modulator (AOM) before the optical pumping region. There we have typically 3-5 mW of laser power available. The radio-frequency  $\nu_{AOM}$  to the AOM is provided by a HP 8656B frequency synthesizer. Rapid switching between different isotopes is achieved by changing  $\nu_{AOM}$ . The typical switching times are limited by the synthesizer to around 50 ms. This procedure reduces the systematic uncertainty of isotope shift measurements due to slow drifts.

The stabilized diode laser system at wavelength  $\lambda_2$  allow to populate the  $^3D$ -states selectively. Around 60% of the Ba atoms decay to the  $^3D_2$  and  $^3D_1$  states and 40% decay back to the ground state. Cycling the  $^1S_0 - ^3P_1$  transition populates the  $^3D$ -states with a ratio of 70% in the  $^3D_2$  and 30% in the  $^3D_1$  states (Tab. 1). At the saturation intensity of  $65 \mu\text{W}/\text{cm}^2$  an interaction length of about 30 mm is sufficient to transfer more than 95% of the atoms in the atomic beam into the metastable states. The laser is stabilized within a fraction of the experimental linewidth. In the experiment we observed a linewidth of the  $^1S_0 - ^3P_1$  transition as low as 2 MHz. It is limited by residual Doppler shifts in the divergent atomic beam, but it is sufficient for good isotope selectivity.

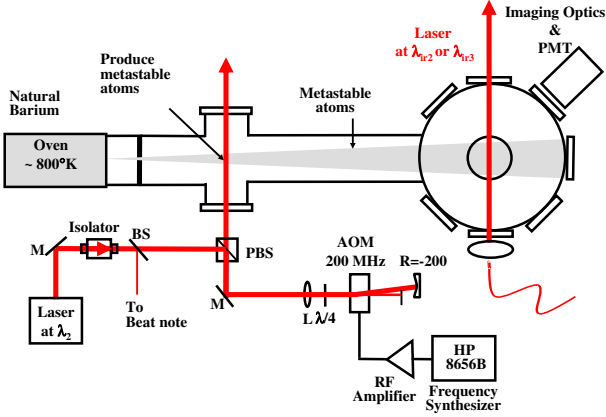


**Fig. 2.** Setup for isotope shift measurements using a beam of metastable Ba atoms. In the first interaction zone, atoms are optically pumped into metastable D-states with laser light at  $\lambda_0=791.3$  nm. A second interaction zone allows to probe the

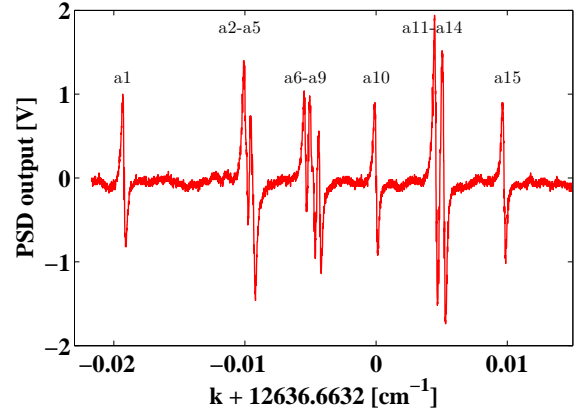


**Fig. 4.** Measured first-derivative hyperfine spectrum of P(52)(0-15) transition in  $^{127}\text{I}_2$  by frequency modulation saturated absorption spectroscopy. We resolve the close lying multiplets from which we determine a resolution of an individual line to 9 MHz. We use the 'a1' component as the reference frequency.

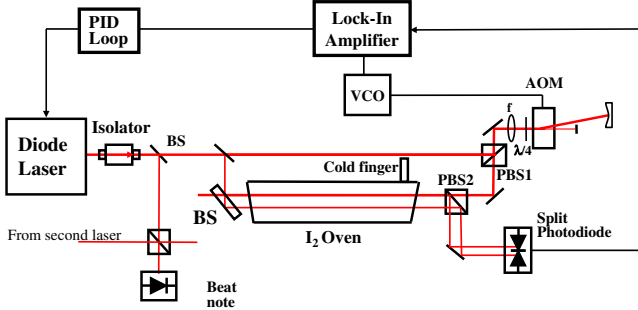


**Fig. 3.** Setup for frequency modulation saturated absorption spectroscopy of iodine  $^{127}\text{I}_2$ . The laser beams have linear polarization. The pump beam polarization is orthogonal to the polarization of the two probe beams. The pump beam is frequency modulated with a double passed AOM. The difference signal between the two probe beams is detected on a balanced split photodetector.

In the course of the measurements we determined the absolute frequency of the  $^1S_0$ - $^3P_1$  transition in  $^{138}\text{Ba}$ . The transition is located  $-611(3)$  MHz below the 'a1' iodine line, which is at  $12636.64357(1)$   $\text{cm}^{-1}$  [18,19]. Our determination is a factor 100 better and within the uncertainty of  $0.001$   $\text{cm}^{-1}$  of previous measurements [20].

## 2.2 Laser spectroscopy of D-states

We use custom built fiber laser systems by KOHERAS for probing the  $^3D$ -states. The laser wavelengths can be temperature tuned by about 0.4 nm and piezo tuned by about 0.3 nm. For changing the laser frequency during the measurements we used the piezo, while we kept the temperature constant. The observed thermal drift of the lasers was less than 50 MHz/h. The transitions are always detected through fluorescence at  $\lambda_1$  from the  $^1P_1$  -  $^1S_0$

transition which can be detected with a standard photomultiplier tube (Hamamatsu R7205-01).

## 3 Isotope shift of the $^3D-^1P_1$ transitions

We investigate the isotope shifts of the transitions from the  $^3D_1$  and  $^3D_2$ -state, because they are sensitive to electron correlations and to coupling to nuclear parameters. The  $^3D_1-^1P_1$  transition is the weakest among the three repumping transitions for laser cooling of Ba. In the experimental procedure, the known isotope shift [17] and hyperfine structure [21] of the  $^3P_1$  level (Tab. 3) were used to select different isotopes. The measurements are summarized in Table 5.

### 3.1 Even isotopes

Because of the absence of nuclear spin there is no hyperfine structure for even isotopes. For measurements with these systems the frequency of the diode laser at  $\lambda_2$  is toggled between two different isotopes by switching the frequency  $\nu_{AOM}$ . In this way we probe both isotopes before we change the frequency of the fiber laser at  $\lambda_{ir3}$  (Fig. 5). The fitted linewidth is  $33(3)$  MHz for all resonances. The separation of the resonances for the different isotopes at  $\lambda_{ir3}$  is of the order of the natural linewidth. Without isotope selective population of the D-states the determination of the line center would require much higher statistics. The signal amplitude is proportional to the natural abundance of the isotopes. We find from the peak intensities the abundance ratio  $^{138}\text{Ba} : ^{136}\text{Ba}$  to  $10.0(4):1$ , and  $^{136}\text{Ba} : ^{134}\text{Ba}$  to  $3.1(2):1$ , which is in good agreement with the natural abundances.

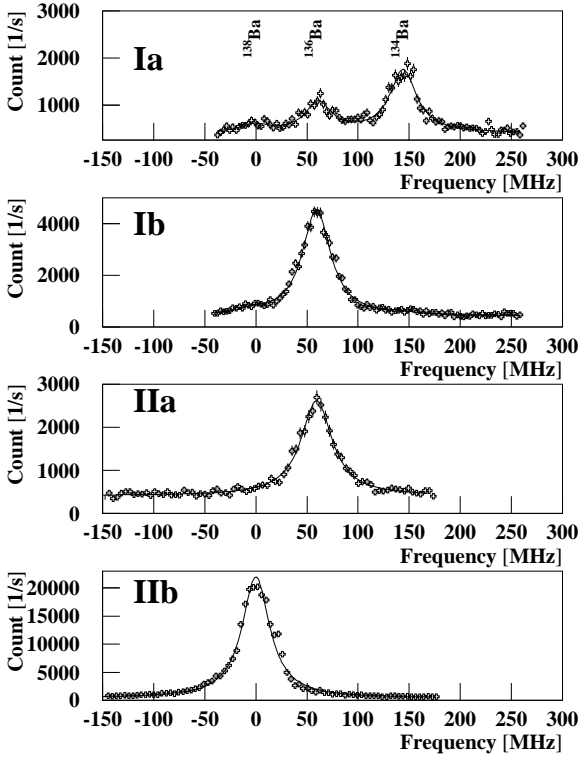


**Fig. 5.** Isotope shift for  $^{138}\text{Ba}$ ,  $^{136}\text{Ba}$ ,  $^{134}\text{Ba}$  at wavelength  $\lambda_{ir3}$ . Spectra Ia and Ib, respectively IIa and IIb, are taken simultaneously. (Ia) Selecting  $^{134}\text{Ba}$ . Because the isotope shift at wavelength  $\lambda_2$  of the pumping transition is small, we populate also the other isotopes at the same time. (Ib) and (IIa) Selecting  $^{136}\text{Ba}$  and (IIb)  $^{138}\text{Ba}$ . The strength of the signal scales with the natural abundance of the selected isotope. A Lorentzian lineshape is fitted to the resonances. The frequency can be given relative to the transition in  $^{138}\text{Ba}$ .

### 3.2 Odd isotopes

In the odd isotopes we have hyperfine structure multiplets. The hyperfine levels in the triplet D-states are populated by locking the diode laser to the  $^1S_0(F=3/2) - ^3P_1(F=3/2)$  transition, which is shifted by  $-925.6(1.0)$  MHz relative to the transition in  $^{138}\text{Ba}$ . The selection rules allow to populate the  $F=1/2, 3/2$  and  $5/2$  states of the  $^3D_1$  level for  $^{137}\text{Ba}$  and  $^{135}\text{Ba}$ .

The hyperfine structure splitting of the  $^3P_1$  state in Ba isotopes with nuclear spin  $I=3/2$  has been measured before with high accuracy by optical-rf double-resonance, using a hollow cathode lamp as a light source [21]. The hyperfine structure of the  $^3D_1$  state was determined by an atomic beam magnetic resonance method [22].

We have measured the hyperfine spectrum of  $^{137}\text{Ba}$  and  $^{135}\text{Ba}$  isotopes for the  $^3D_1 - ^1P_1$  transition simultaneously by selecting the isotopes through optical pumping using the intercombination line. The laser frequency at  $\lambda_{ir3}$  is scanned over the entire set of hyperfine lines which are spread over more than 2 GHz (Fig. 6). All the seven transitions can be fitted with a sum of Lorentzian func-

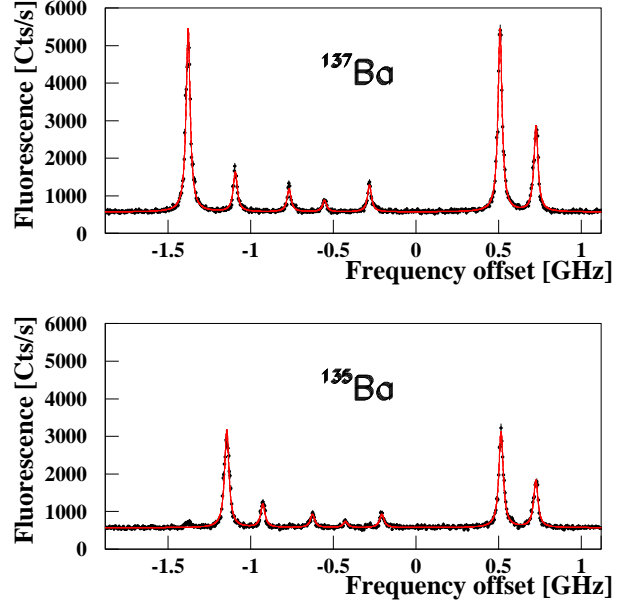


**Fig. 6.** Measured hyperfine spectra for the  $^3D_1 - ^1P_1$  transition for  $^{137}\text{Ba}$  and  $^{135}\text{Ba}$ . The frequency axis is relative to the same transition in  $^{138}\text{Ba}$ . Each frequency point was measured for 1 second.

tions

$$F_\nu = C + \sum_{i=1}^7 \frac{A_i}{1 + (\frac{\nu - \nu_i}{\Gamma/2})^2}, \quad (1)$$

where  $C$  represents the background counts,  $i$  is the index of the hyperfine components,  $A_i$  is the amplitude of each component,  $\Gamma$  is the full width at half maximum and  $\nu_i$  is the center of the hyperfine component. From the fit we obtain  $\Gamma = 20(1)$  MHz, which is in good agreement with the natural linewidth of the transition.

We derived the isotope shift between the isotopes  $^{137}\text{Ba}$  and  $^{135}\text{Ba}$  from the measured hyperfine spectra. We determine the difference frequencies  $\Delta\nu_1$  (Tab. 4) of all seven hyperfine components. With the known hyperfine splittings of the  $^3D_1$  [22] and  $^1P_1$ -states [9] we calculate the difference  $\Delta\nu_2$  for all hyperfine transitions of the two isotopes. Thus, the isotope shift  $\Delta\nu_{IS}$  is

$$\Delta\nu_{IS} = \Delta\nu_1 + \Delta\nu_2, \quad (2)$$

where the difference in the hyperfine structure  $\Delta\nu_2$  for the two isotopes is

$$\Delta\nu_2 = [\Delta\nu_{hfs}(^3D_1)\Delta\nu_{hfs}(^1P_1)]_{137} \quad (3)$$

$$-[\Delta\nu_{hfs}(^3D_1) - (\Delta\nu_{hfs}(^1P_1))]_{135}. \quad (4)$$

We note that the error is smallest where the transitions nearly coincide in frequency ( $(5/2 \rightarrow 5/2)$  and  $(5/2 \rightarrow 3/2)$ ). Here, the effect of the uncertainty of the frequency calibration of the fiber laser is minimal. The average over all seven values for  $\Delta\nu_{IS}$  yields an isotope shift of  $-75.3(5)$  MHz between  $^{137}\text{Ba}$  and  $^{135}\text{Ba}$ .

Odd isotopes: $^3D_{1-1}P_1$ transition			
Transition	$\Delta\nu_1$ [MHz]	$\Delta\nu_2$ [MHz]	$\Delta\nu_{IS}$ [MHz]
1/2→3/2	-229.3(3.3)	151.0(0.4)	-78.4(3.3)
1/2→1/2	-167.3(2.5)	97.8(0.6)	-69.5(2.6)
3/2→5/2	-143.2(2.6)	62.1(0.3)	-81.1(2.6)
3/2→3/2	-128.3(4.2)	53.8(0.4)	-74.4(4.2)
3/2→1/2	-76.2(2.2)	0.7(0.6)	-75.5(2.3)
5/2→5/2	-6.1(0.6)	-68.5(0.3)	-74.6(0.7)
5/2→3/2	1.2(1.0)	-76.7(0.4)	-75.5(1.1)

**Table 4.** Isotope shifts between  $^{137}\text{Ba}$  and  $^{135}\text{Ba}$  for the  $6s5d\ ^3D_1 - 6s6p\ ^1P_1$  transition. The measured frequency difference  $\Delta\nu_1$  of corresponding hyperfine transitions and the difference in the hyperfine splitting  $\Delta\nu_2$  of the involved states from literature [9, 22] are given.

Isotope pair	$^3D_{1-1}P_1$ [MHz]	$^3D_{2-1}P_1$ [MHz]
138-136	-59.3(6)	-63(1)
138-134	-144.1(1.0)	-143(1)
136-134	-84.8(8)	-80(1)
138-137	114(4)	69(3)
138-135	39(4)	
137-135	-75.3(5)	

**Table 5.** Isotope shifts for the  $6s5d\ ^3D_{1,2} - 6s6p\ ^1P_1$  transition in Ba isotopes. The uncertainty for the shift between odd and even isotopes is systematically larger due to the uncertainty in the frequency calibration of the fiber laser.

## 4 Analysis of isotope shifts

The isotope shift of an atomic transition frequency between two different isotopes of an atom with mass numbers  $A_1$  and  $A_2$  is traditionally written as a sum of normal mass shift ( $\delta\nu_{NMS}$ ), specific mass shift ( $\delta\nu_{SMS}$ ) and field shift ( $\delta\nu_{FS}$ ) [9]

$$\delta\nu_{IS} = \delta\nu_{NMS} + \delta\nu_{SMS} + \delta\nu_{FS}. \quad (5)$$

The normal mass shift arises from the reduced mass correction to the energy levels in an atom and is

$$\delta\nu_{NMS} = \nu \frac{m_e}{m_p} \frac{A_1 - A_2}{A_1 A_2}, \quad (6)$$

where  $m_e$  is the electron mass,  $m_p$  is the proton mass and  $\nu$  is the transition frequency. The specific mass shift is caused by momentum correlation among orbital electrons and is

$$\delta\nu_{SMS} = F_{SMS} \nu \frac{A_1 - A_2}{A_1 A_2}, \quad (7)$$

where  $F_{SMS}$  is a constant for a specific transition and it is insensitive to the nuclear moments. It can be derived from theory.

The field shift arises due to the change in the spatial distribution of the nuclear charge between the different isotopes and is

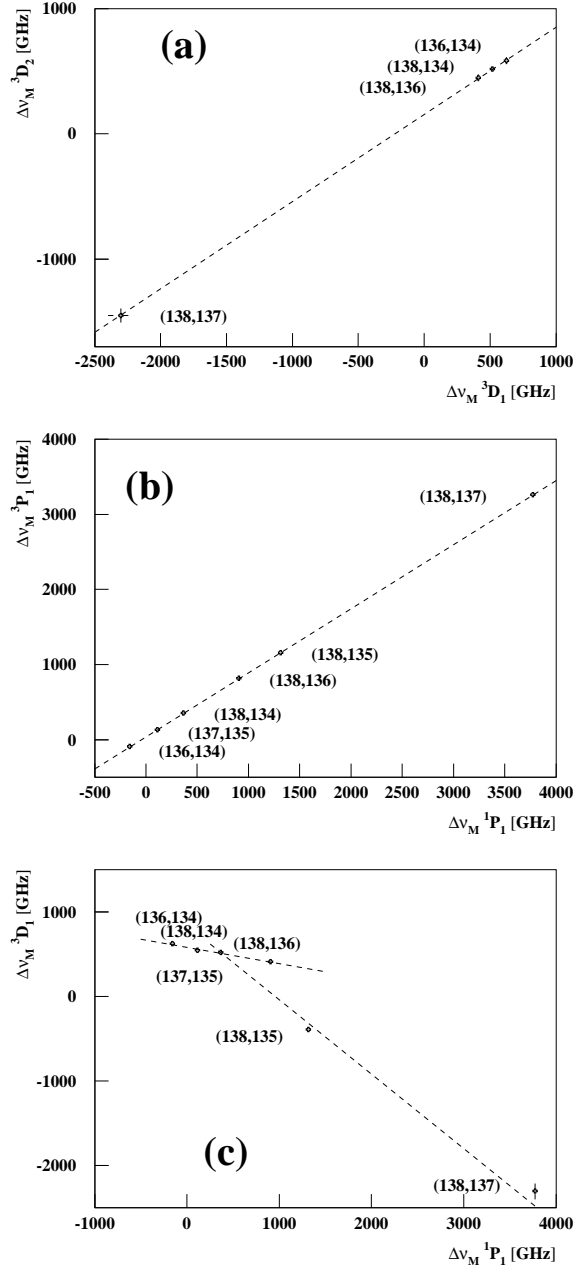


**Fig. 7.** King plot for the measured modified isotope shifts  $\Delta_M$  of the  $^3D_{1-1}P_1$  and  $^3D_{2-1}P_1$  transitions in Ba isotopes. A linear correlation is found for the transitions at the wavelengths  $\lambda_{ir2}$  and  $\lambda_{ir3}$  (a) as well as at the wavelengths  $\lambda_1$  and  $\lambda_2$  (b). For the the wavelength pair  $\lambda_{ir2}$  and  $\lambda_1$  we find a deviation (c). There is a linear dependence for pairs of even-even isotopes which differs from the relation for odd-odd and even-odd pairs of isotopes. The data for  $\lambda_1$  and  $\lambda_2$  are taken from [17].

$$\delta\nu_{FS} = F\delta\langle r^2 \rangle, \quad (8)$$

where  $F$  is a factor depending on the electronic configuration and  $\langle r^2 \rangle$  is the expectation value of the square of the radius of the charge distribution in the nucleus. This term provides information on the overlap of the electron wavefunctions with the nucleus.

Isotope shifts for different transitions are often compared using a King plot [23]. Here, the modified isotope shifts  $\Delta\nu_M$ , which is given as

$$\Delta\nu_M = (\Delta\nu_{IS} - \Delta\nu_{NMS}) \times \frac{A_1 A_2}{A_1 - A_2}, \quad (9)$$

of a set of isotope pairs is plotted for two different transitions. The King plot is expected to exhibit a linear dependence relating the two isotope shift pair values. The slope gives the ratio of field factors  $F_{SMS}$  for the two transitions and the intercept is related to the difference in specific mass shifts. Figure 7 gives King plots for the isotope shifts of the  $^3D_{1,2}-^1P_1$  and  $^3D_{2,1}-^1P_1$  transitions. A linear correlation with a slope of 0.696(20) is found for the modified isotope shift  $\Delta\nu_M$  for the 5d-6p transitions at the wavelengths  $\lambda_{ir2}$  and  $\lambda_{ir3}$  (Fig. 7a). The linear dependence for the 6s-6p transitions at wavelength  $\lambda_1$  and  $\lambda_2$  has a slope of 0.852(6) (Fig. 7b). It appears that in the studied  $^3D_{1,2}-^1P_1$  transitions the dominant single electron contribution arises from a 5d-6p transition in contrast to all other reported isotope shift measurements in this systems, where stronger 5s-6p transitions were involved. The modified isotope shift  $\Delta\nu_M$  for transitions with the same dominant single electron contribution exhibit the expected linear correlation.

The situation is different for the 5d-6p transition at wavelength  $\lambda_{ir3}$  and the 6s-6p transition at wavelength  $\lambda_1$ . For this transition pair we find a deviation from a linear dependence (Fig. 7c). A linear correlation is only seen for the subsets of even-even isotope pairs and subset of isotope pairs involving odd isotopes. The slope for even-even pairs of isotopes is -0.191(8), while the slope for odd-odd together with the even-odd pairs is -0.88(2). This indicates that the nuclear spin effects the electron-electron correlations and gives rise to an additional contribution to the isotope shift for atoms with nuclear spin.

We note that, similar to our observation, there are instances of deviation from a linear function, e.g., in Samarium isotopes [24]. The deviations may be due to electron-electron correlation in two electron systems. The nuclear charge radius contribution is not prominent. There are no theoretical calculations yet to compare our results with.

## 5 Conclusions

In this work precision spectroscopy of the metastable D-states is reported. It yielded the first time measurement of isotope shifts of the  $^3D_{1,2}-^1P_1$  transitions and optically resolved hyperfine structure. The parameters obtained in the spectroscopy of these states is essential input for effective laser cooling of heavy alkaline earth systems. The established transition rates for these weak transitions involved are sufficient to allow for repumping in a laser cooling scheme.

The measurements contribute to the understanding of the atomic structure of heavy alkaline earth elements. In particular they can be exploited as input for atomic structure calculations which is in progress in several groups [5].

The isotope shifts of the 5d-6p  $^3D_{1,2}-^1P_1$  transitions cannot be scaled from other measurements which were performed on 6s-6p transitions. In particular, the  $^3D$ -states seem to couple to the nuclear parameters, which can be also seen in the large hyperfine structure splitting, which is caused by so-called core-polarization [25]. A solution of this discrepancy by future theoretical work is needed in order to have the necessary reliable wavefunction for heavy alkaline earth elements for, e.g. enhancement factor calculations in edm search projects.

## 6 Acknowledgements

We would like to thank B. Sahoo for helpful discussions on the issue of isotope shifts. This work was supported by the *Nederlandse Wetenschappelijke Organisatie (NWO)* by and NWO-VIDI grant, and the *Stichting voor Fundamenteel Onderzoek der Materie (FOM)* under programme 48 (TRI $\mu$ P).

## References

1. V. V. Flambaum, Phys. Rev. A 60, R2611 (1999).
2. V.A. Dzuba, V.V. Flambaum and J.S.M. Ginges, Phys. Rev. Lett. **A61**, 062509 (2000).
3. J. Engel, J.L. Friar, and A.C. Hayes, Phys. Rev. C **61**, 035502 (2000); J. Dobaczewski and J. Engel, Phys. Rev. Lett. **94**, 232502 (2005).
4. V.A. Dzuba, V.V. Flambaum, J.S.M. Ginges, and M.G. Kozlov, Phys. Rev. **A66**, 012111 (2002); V.V. Flambaum and V.G. Zelevinsky, Phys. Rev. C **68**, 035502 (2003).
5. Groups at the University of Southwest Wales (V. Flambaum et al.), at Warsaw University (K. Pachucki et al.), and at Krakow University (J. Bieroń) develop and improve independent numerical codes for heavy atomic systems, (e.g. J. Bieroń, C. Froese Fischer, S. Fritzsche, and K. Pachucki, J. Phys. B: At. Mol. Opt. Phys. 37 305 (2004)). The calculations aim at a better understanding of atomic parity violation and other symmetry violating contributions on the atomic structure. Private communications.
6. J.R. Guest, N.D. Scielzo, I. Ahmad, K. Bailey, J.P. Greene, R.J. Holt, Z.-T. Lu, T.P. O'Connor, and D. H. Potterveld, Phys. Rev. Lett. **98** 093001 (2007).
7. K. Jungmann, Proc. Heavy Quarks and Leptons, HQL06, S. Recksiegel, A. Hoang, and S. Paul (Eds), e-conference C0610161, 331 (2006).
8. K. Jungmann, Acta Phys. Pol. B 33, 2049 (2002); E. Traykov et al., arXiv:0709.3670 (2007).
9. W. A. van Wijngaarden and J. Li, Can. J. Phys., 73, 484 (1995).
10. H.Katori, T. Ido, Y. Isoya, and M. Kuwata-Gonokami, Phys. Rev. Lett., 82, 1116 (1999).
11. S. Niggli and M. C. E. Huber, Phys. Rev. A 35, 2908 (1987).
12. A. Bizzarri and M. C. E. Huber, Phys. Rev. A 42, 5422 (1990).
13. J. Brust and A. C. Gallagher, Phys. Rev. A 52, 2120 (1995).
14. A. Lurio, Phys. Rev., A 376, 136 (1963).

15. J. Migdalek and W. E. Baylis, Phys. Rev. A 42, 6897 (1990).
16. N. D. Scielzo, J. R. Guest, E. C. Schulte, I. Ahmad, K. Bailey, D. L. Bowers, R. J. Holt, Z. -T. Lu, T. P. O'Connor and D. H. Potterveld, Phys. Rev. A 73, 010501(R)(2006).
17. P. Grundevik, M. Gustavsson, G. Olsson and T. Olsson, Z. Phys. A 312, 1 (1983).
18. S. Gerstenkorn, J. verges, and J. Chevillard, *Atlas du Spectre D' Absorption de la Molecule D'Iode* (Laboratoire Aime Cotton, Orsay, France, 1982); H. Knöckel, B. Bodermann, and E. Tiemann, Eur. Phys. J. D 28, 199 (2004).
19. Accuracy of an individual line in this region of the I<sub>2</sub> spectrum is expected to be better than 0.1 MHz, H. Knöckel, private communication.
20. J.J. Curry, J. Phys. Chem. Ref. Data 33, 725 (2004).
21. G. zu Putlitz, Ann. Phys., 11, 248 (1963).
22. M. Gustavsson, G. Olsson and A. Rosén, Z. Phys. A 290, 231 (1979).
23. W. H. King, J. Opt. Soc. Am., 53, 638 (1963).
24. J. A. R. Griffith, G. R. Isaak, R. New and M. P. Ralls, J. Phys. B: At. Mol. Phys., 14, 2769 (1981).
25. B. Sahoo, C. Sur, T. Beier, B.P. Das, R.K. Chaudhuri, and D. Mukherjee, Phys. Rev. A 75, 042504 (2007).